Supporting Information for:

Liver X Receptor Controls Follicular Helper T Cell Differentiation via Repression of TCF-1

Jiyeon Kim, Haeseung Lee, Jeong-Eun Lee, Garam Choi, Hayeon Chung, Daehong Kim, Min Jung Park, Yong Seok Gye, Kwang-Soo Shin, Chang-Yuil Kang, Seung-Ki Kwak, and Yeonseok Chung*

*Correspondence:

Yeonseok Chung

Email: yeonseok@snu.ac.kr

This PDF file includes:

Supplementary materials and methods

Mice

C57BL/6 mice were purchased from Orient Bio (Seongnam, Republic of Korea). B6.SJL, *Rag1*$^{-/-}$, and OT-II mice were purchased from The Jackson Laboratory (Bar Harbor, ME, USA). *Nr1h2*$^{-/-}$ mice were kindly provided by Dr. Won-Il Jeong (KAIST, Republic of Korea). *Nr1h3*$^{-/-}$mice were kindly provided by Dr. Sang Geon Kim (Dongguk University, Republic of Korea). All mice were used at 6-10 weeks of age and maintained in the Animal Center for Pharmaceutical Research of Seoul National University under specific pathogen-free conditions.

In vitro helper T cell differentiation

Flow-sorted naive CD4$^+$ T cells were stimulated with plate-coated anti-CD3 (1 μg/mL) and soluble anti-CD28 (1 μg/mL) for 3 days. For Th1 cell differentiation, recombinant mouse IL-2 (2 ng/mL; eBioscience) and recombinant mouse IL-12 (10 ng/mL; Peprotech) were added. For Th2 cell differentiation, recombinant mouse IL-2 (10 ng/mL) and recombinant mouse IL-4 (10 ng/mL; Peprotech) were added. For Th17 cell differentiation, recombinant human TGFß (1 ng/mL; Peprotech), and recombinant mouse IL-6 (50 ng/mL; Peprotech) were added. For Treg cell differentiation, recombinant mouse IL-2 (20 ng/mL), and recombinant human TGFß (5 ng/mL) were added. For Tfh-like cell differentiation, anti-CD3ε (145-2C11, 1 μg/mL) and anti-CD28 (37.51, 1 μg/mL) (BioXcell) Abs were used to precoat a 96-well flat-bottom plate (Corning, USA) overnight at 4 °C. Naïve OT-II cells were cultured with recombinant mouse IL-6 (50 ng/mL) (PeproTech, USA), anti-IFNγ (XMG1.2), anti-IL4 (11B11), and anti-TGFß (1D11) neutralizing antibodies (all from BioXCell, USA) for 3 days. For Tfh-like cell activation, Tfh-like cells were cultured with $Ova_{323-339}$ in the presence of T-cell depleted splenocytes. In some experiments, cells were treated with either DMSO vehicle or 1 μM GW3965.

Tfh-B cell co-culture Assay

Mice were immunized with KLH in CFA and draining lymph nodes were harvested and pooled, teased into single-cell suspensions, followed by CD4 MACS enrichment (Miltenyi Biotec). Enriched samples were identified and FACS-sorted for Tfh cells as CD3e$^+$CD4$^+$CXCR5$^+$PD-1$^+$. Naïve B cells from wild-type mice were sorted as B220$^+$IgD$^+$GL7$^-$. Tfh cells and naïve B cells were cultured in 3:5 ratio with anti-CD3ε (2 μg/mL) and anti-IgM (5 ug/mL) (Jackson ImmunoResearch Inc., USA). Culture supernatant was analyzed via ELISA for IgG levels 7 days later.

Human CD4$^+$ T cell studies

Human peripheral blood was obtained from healthy volunteers who are not taking any medications. PBMCs were prepared by using a lymphocyte separation medium (MP Biomedicals), according to the manufacturer's instruction. CD4$^+$ T cells were isolated by CD4 MACS enrichment (Miltenyi Biotec). Naive CD4$^+$ T cells were flow-sorted as CD3$^+$CD4$^+$CD45RA$^+$CD45RO$^-$CD25$^-$ and stimulated with plate-coated anti-CD3 (10 μg/mL, OKT3; Biolegend), and soluble anti-CD28 (2 μg/mL, CD28.2; Biolegend). For Tfh cell polarization, recombinant human IL-12 (2 ng/mL; R&D), and recombinant human TGFβ (1 ng/mL) were added and cultured for 4 days. Cells were treated with either DMSO vehicle, 5 μM GW3965, or 1 μM BIO.

Flow cytometry

For intracellular cytokine analysis, cells were stimulated with phorbol 12-myristate 13-acetate (100ng/mL; Sigma-Aldrich) and ionomycin (1 μmol/L; Sigma-Aldrich) plus Brefeldin A and monensin (both from eBioscience) before staining. Intracellular staining was performed using either IC fixation buffer or Foxp3/Transcription factor staining kit (eBioscience). For phospho-protein staining, cells were permeabilized using Perm Buffer III (BD Bioscience). Samples were analyzed with LSRFortessa (BD Biosciences), and data were analyzed using FlowJo software (BD Biosciences). The following antibodies were used for flow cytometric analysis or cell sorting: Alexa Flour 488-conjugated antibodies to mouse IL-4 (11B11; Biolegnd), phospho-Akt (193H12; Cell Signaling Technology), mouse/human TCF-1 (C63D9, Cell Signaling Technology), and Goat anti-Rabbit IgG secondary antibody

(Invitrogen); FITC-conjugated antibody to mouse PD-1 (J43; eBioscience); PE-conjugated antibodies to mouse IgD (11-26c.2a; Biolegend), mouse IL-2 (JES6-5H4; Biolegend), mouse IL-17 (TC11-18H10.1; Biolegend), human CD25 (BC96; Biolegend), mouse/human BCL6 (IG191E/A8; Biolegend), mouse CD95 (15A7, eBioscience), and mouse/human LEF-1 (C12A5, Cell Signaling Technology); Alexa Flour 647-conjugated antibody to mouse/human TCF-1 (C63D9, Cell Signaling Technology), human CD45RO (UCHL1; Biolegend), and human CXCR5 (RF8B2, BD Biosciences); APC-conjugated antibodies to mouse CD25 (PC61; Biolegend), and mouse CD138 (281-2; Biolegend); APC Streptavidin (Biolegend); APC/Cy7-conjugated antibodies to mouse CD38 (90; Biolegend), and human CD3 (OKT3; Biolegend); PerCP/Cy5.5-conjugated antibodies to mouse CD62L (MEL-14; Biolegend), and human CD4 (OKT4; Biolegend); PE/Cy7-conjugated antibodies to mouse/human CD44 (IM7; Biolegend), and mouse IL-13 (2Bio13A, eBioscience); Pacific blue-conjugated antibodies to mouse/human GL7 (GL7, Biolegend), mouse CD4 (GK1.5; Biolegend), human CD45RA (HI100; Biolegend), and mouse CD45.1 (A20, Biolegend); V450-conjugated antibody to mouse S6 (N7-540; BD Biosciences); eFlour 450-conjugated antibody to FOXP3 (FJK-165, eBioscience); BV605-conjugated antibody to mouse CD69 (H1.2F3; Biolegend); BV711-conjugated antibody to mouse IFNγ (XMG1.2; Biolegend); BUV395-conjugated antibodies to mouse CD8a (53-6.7; BD Biosciences), mouse B220 (RA3-6B2; BD Biosciences), and mouse CD45.2 (104, BD Biosciences); BUV737-conjugated antibody to mouse CD4 (GK1.5; BD Biosciences); Biotin-conjugated antibody to mouse CXCR5 (L138D7; Biolegend); phospho-MAPK (D13.14.4E; Cell Signaling Technology, and phospho-GSK3β (D85E12; Cell Signaling Technology). In certain experiments, Fixable Viability Dye, CellTrace™ Violet Cell Proliferation Kit, Vybrant™ CFDA SE Cell Tracer Kit, BODIPY™ 493/503 (ThermoFisher Scientific, MA, USA), or Filipin III (Sigma-Aldrich) were employed according to the manufacturer's instructions.

Quantitative real-time PCR

Total RNA was extracted by using TRIzol (Thermo Fisher Scientific, USA), and cDNA was synthesized with a RevertAid First Strand cDNA Synthesis Kit (ThermoFisher) according to the manufacturer's instructions. Gene expression was measured using iTaq Universal SYBR Green Supermix (Bio-rad, USA) and Applied Biosystems 7500 Fast real-time PCR system (Thermo Fisher Scientific). Primers for mouse *Actb* (forward: 5′-TGG AAT CCT GTG GCA TCC ATG AAA C-3′, reverse: 5′-TAA AAC GCA GCT CAG TAA CAG TCC G-3′), *Hmgcs1* (forward: 5′-AAA TGC CAG ACC TAC AGG TGG-3′, reverse: 5′-ATG CTG CAT GTG TGT CCC A-3′), *Hmgcr* (forward: 5′-GAA TGC CTT GTG ATT GGA GTT G -3′, reverse: 5′-ACA CAG GCC GGG AAG AAT G-3′), *Pmvk* (forward: 5′-GTA GTG GCC TCG GAG CAG AGT CGA CAG C -3′, reverse: 5′-GTG GTT CTC AAT GAC CCA GTC AAA GTT CCC-3′), *Fdft1* (forward: 5′-GGA TGT GAC CTC CAA ACA GGA C-3′, reverse: 5′-CAG ACC CAT TGA GTT GGC ACA C-3′), *Sqle* (forward: 5′-TGT TGC GGA TGG ACT CTT CTC C-3′, reverse: 5′-GTT GAC CAG AAC AAG CTC CGC A-3′), *Cyp51* (forward: 5′-ATC CAG AAG CGC AGG CTG TCA A-3′, reverse: 5′-CAG TCC GAT GAG CAT CCC TGA T-3′), *Nsdhl* (forward: 5′-TTA ACC GCA GCC ATT CGT CCT C-3′, reverse: 5′-GGT GAA GTC CAC CAG GTT TTC C-3′), *Dhcr7* (forward: 5′-CAA GAC ACC ACC TGT GAC AGC T-3′, reverse: 5′-CTG CTG GAG TAA TGG CAC CTT C-3′), *Sult2b1a* (forward: 5′-GCA GTT TGG CTC CTG GTT TGA C-3′, reverse: 5′-CCA GGA ACT CAC AGA TGC GTT G-3′), *Cyp11a1* (forward: 5′-TGC TCA ACC TGC CTC CAG ACT T-3′, reverse: 5′-ACT GGC TGA AGT CTC GCT TCT G-3′), *Cyp27a1* (forward: 5′-CAA CCT CCT TTG GGA CTT AC -3′, reverse: 5′-TGA TCC ATG TGG TCT CTT ATT G-3′), *Srebf2* (forward: 5′-CCA AAG AAG GAG AGA GGC GG-3′, reverse: 5′-CGC CAG ACT TGT GCA TCT TG-3′), *Nr1h2* (forward: 5′-CGC TAC AAC CAC GAG ACA GA-3′, reverse: 5′-TGT TGA TGG CGA TAA GCA AG-3′), *Nr1h3* (forward: 5′-TGG GAT GTC CAC GAG TGA CTG TTT-3′, reverse: 5′-TCC CTT AAT GCT ACG GAA GGC TCT-3′), *Rxra* (forward: 5′-ATG GAC ACC AAA CAT TTC CTG C-3′, reverse: 5′-CCA GTG GAG AGC CGA TTC C3′), *Rxrb* (forward: 5′-GCC CAA ATG ACC CAG TGA CTA-3′, reverse: 5′-CTT TGC CCA CTC AAC GAG TGT-3′), *Il21* (forward: 5′-TCA TCA TTG ACC TCG TGG CCC-3′, reverse: 5′-ATC GTA CTT CTC CAC TTG CAA TCC C-3′), *Tcf7* (forward: 5′-CGA GAA GAG CAG GCC AAGTA-3′, reverse: 5′-CCT GTG GTG GAT TCT TGA TG-3′), *Abca1* (forward: 5′- AGT GAT AAT CAA AGT CAA AGG CAC AC-3′, reverse: 5′- AGC AAC TTG GCA CTA GTA ACT CTG-3′), and *Abcg1* (forward: 5′- TTC ATC GTC CTG GGC ATC TT-3′, reverse: 5′- CGG

ATT TTG TAT CTG AGG ACG AA-3′) were purchased from Macrogen (Seoul, Republic of Korea). Relative gene expression was normalized to the expression of β-actin (Actb).

ELISA

ELISA was conducted as described previously (1). Briefly, to measure the levels of KLH-specific Ig levels in serum, samples were serial diluted using 1% BSA/PBS and loaded onto KLH-coated ELIA plates (Thermo) detected with HRP-conjugated detection antibody for total IgM (1020-05), IgG (1010-05), IgG1 (1070-05) or IgG2c (1079-05) (all from SouthernBiotech, USA). To measure NP-specific Ig levels in serum, samples were loaded onto NP-BSA (Ratio 5-9 or >20, all from Biosearch Technologies)-coated ELISA plates. To measure the total IgG levels in culture supernatants, IgG was quantified with a total Ig capture antibody (Goat anti-mouse Ig, Human ads-UNLB, 1010-01, SouthernBiotech) and HRP-conjugated detection antibody for IgG.

RNA-seq analysis

Wild type and *Nr1h2*$^{-/-}$ mice were infected with LCMV-Armstrong and spleens were harvested and pooled, teased into single-cell suspensions, followed by CD4 MACS enrichment (Miltenyi Biotec). Enriched samples were identified and FACS-sorted for Tfh as CD3e^{+}CD4^{+}CXCR5^{+}PD-1^{+}. Total RNA was isolated from cells according to the manufacturer's instructions (mirVana miRNA Isolation Kit) and mRNA sequencing libraries were prepared according to the manufacturer's instructions (Illumina Truseq stranded mRNA library prep kit). The quality of sequencing reads was checked using FastQC (v0.11.9). TrimGalore (v0.6.5) was used to remove poor quality bases (Phred score < 20) and the common regions of the Illumina adapter sequences. The cleaned reads were mapped to the mouse genome assembly GRCm38 (mm10) using the STAR aligner (v2.7.3a) with default settings. Transcript abundance per gene, such as expected read count or transcripts per million (TPM), was quantified by RSEM (v1.3.3) with mouse gene annotation GRCm38.86. The raw sequence data (FASTQ files) and pre-processed count data were deposited in the Gene Expression Omnibus with accession number GSE224303. Differential gene expression analysis between the groups (e.g., KO vs. WT) was performed using the edgeR package (v3.38) in R (v3.6.3).

Statistical analysis

Data were analyzed with GraphPad Prism 9 (GraphPad Software; CA, USA). P values were determined using a two-tailed Student's t-test and are presented within each figure and figure legend. Values of $P < 0.05$ were considered statistically significant.

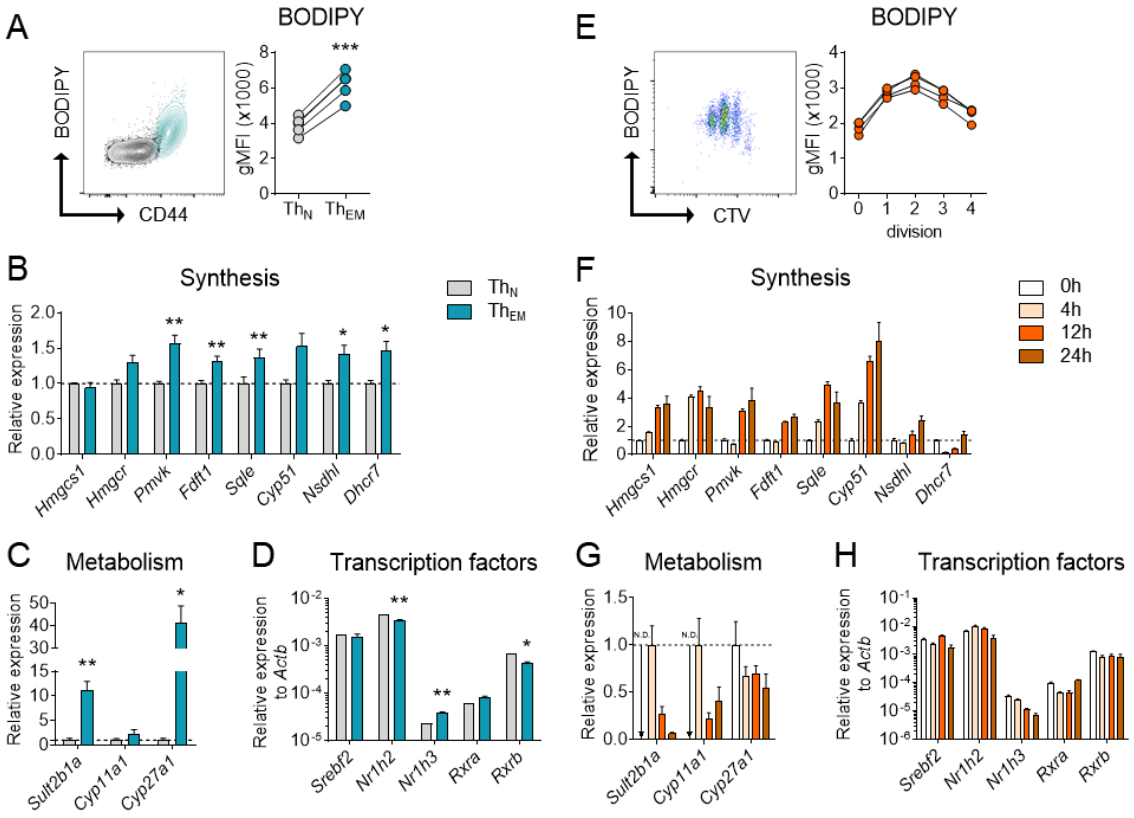

Figure S1. Cholesterol metabolism is regulated by CD4⁺ T cell activation.
(A) Expression of BODIPY493/503 of naïve CD4⁺ T cells and effector memory CD4⁺ T cells (n=5). (B-D) Naïve CD4⁺ T cells and effector memory CD4⁺ T cells were sorted, and relative gene expression was analyzed by qRT-PCR (n=4). (E) CTV-labeled naïve CD4⁺ T cells were stimulated with anti-CD3 and anti-CD28. Expression of BODIPY493/503 according to the number of divisions (n=4). (F-H) CD4⁺ T cells were stimulated with anti-CD3 and anti-CD28 for 0, 4, 12, 24 hours, and relative gene expression was analyzed by qRT-PCR (n=3~4). Data are representative of at least two independent experiments. Quantification plots show the mean ± SEM; *$p < 0.05$, **$p < 0.01$, and ***$p < 0.001$.

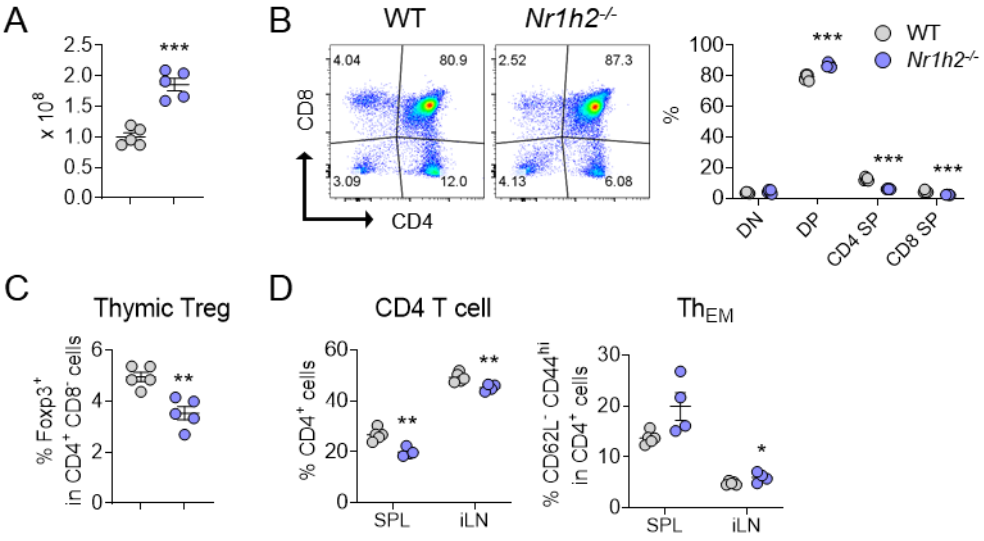

Figure S2. T cell development in *Nr1h2*$^{-/-}$ mice.
(A-C) Analysis of thymocytes at steady-state of WT and *Nr1h2*$^{-/-}$ mice. (A) Absolute cell number of the thymus (n=5). (B) Frequencies of DN, DP, CD4 SP, and CD8 SP populations. (C) Frequency of Foxp3^{+} cells among CD4 SP cells. (D) Frequencies of CD4^{+} T cells, and effector memory CD4^{+} T cells. Data are representative of three independent experiments (n=4~5). Quantification plots show the mean ± SEM; **p < 0.01, and ***p < 0.001.

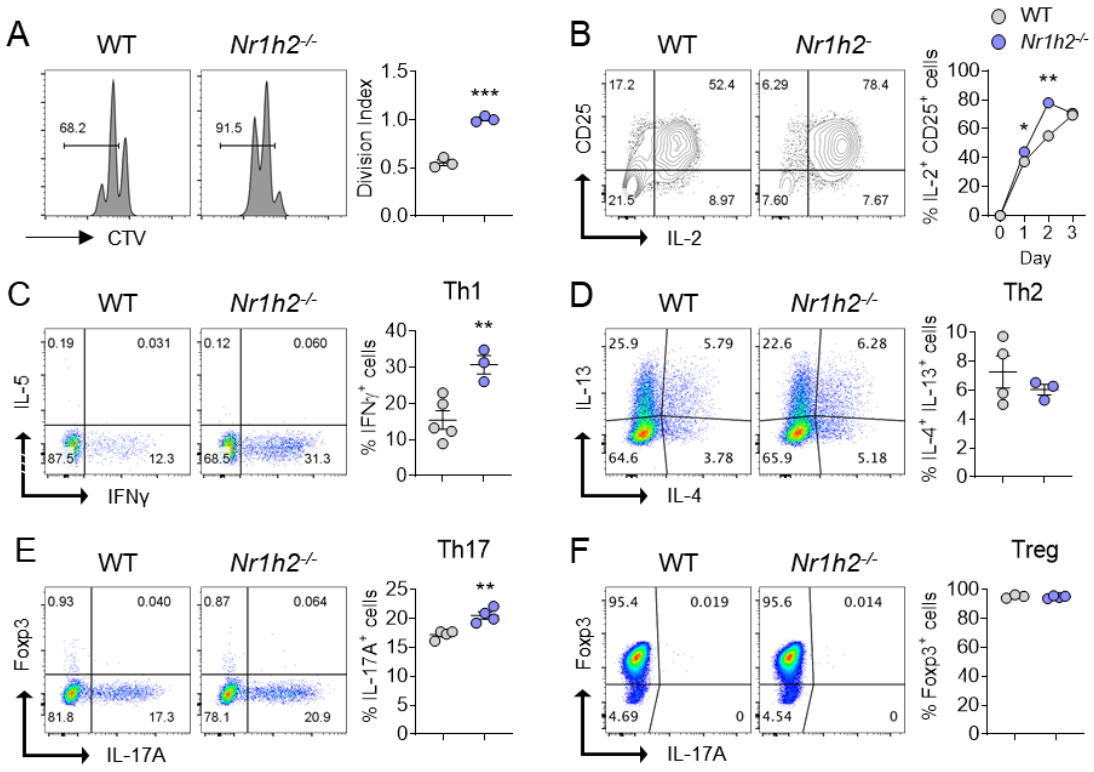

Figure S3. LXR regulates CD4$^+$ T cell differentiation in vitro.
(A-B) Naïve CD4$^+$ T cells from WT and *Nr1h2*$^{-/-}$ mice were stimulated with anti-CD3 and anti-CD28. (A) Calculated division index (n=3). (B) Frequencies of IL-2$^+$CD25$^+$ cells (n=3~4). (C-F) Naïve CD4$^+$ T cells from WT and *Nr1h2*$^{-/-}$ mice were differentiated to Th1, Th2, Th17, and Treg conditions in vitro (n=3-5). (C) Frequencies of IFNγ$^+$ cells. (D) Frequencies of IL-4$^+$IL-13$^+$ cells. (E) Frequencies of IL-17A$^+$ cells. (F) Frequencies of Foxp3$^+$ cells. Data are representative of three independent experiments. Quantification plots show the mean ± SEM; *$p < 0.05$, **$p < 0.01$, and ***$p < 0.001$.

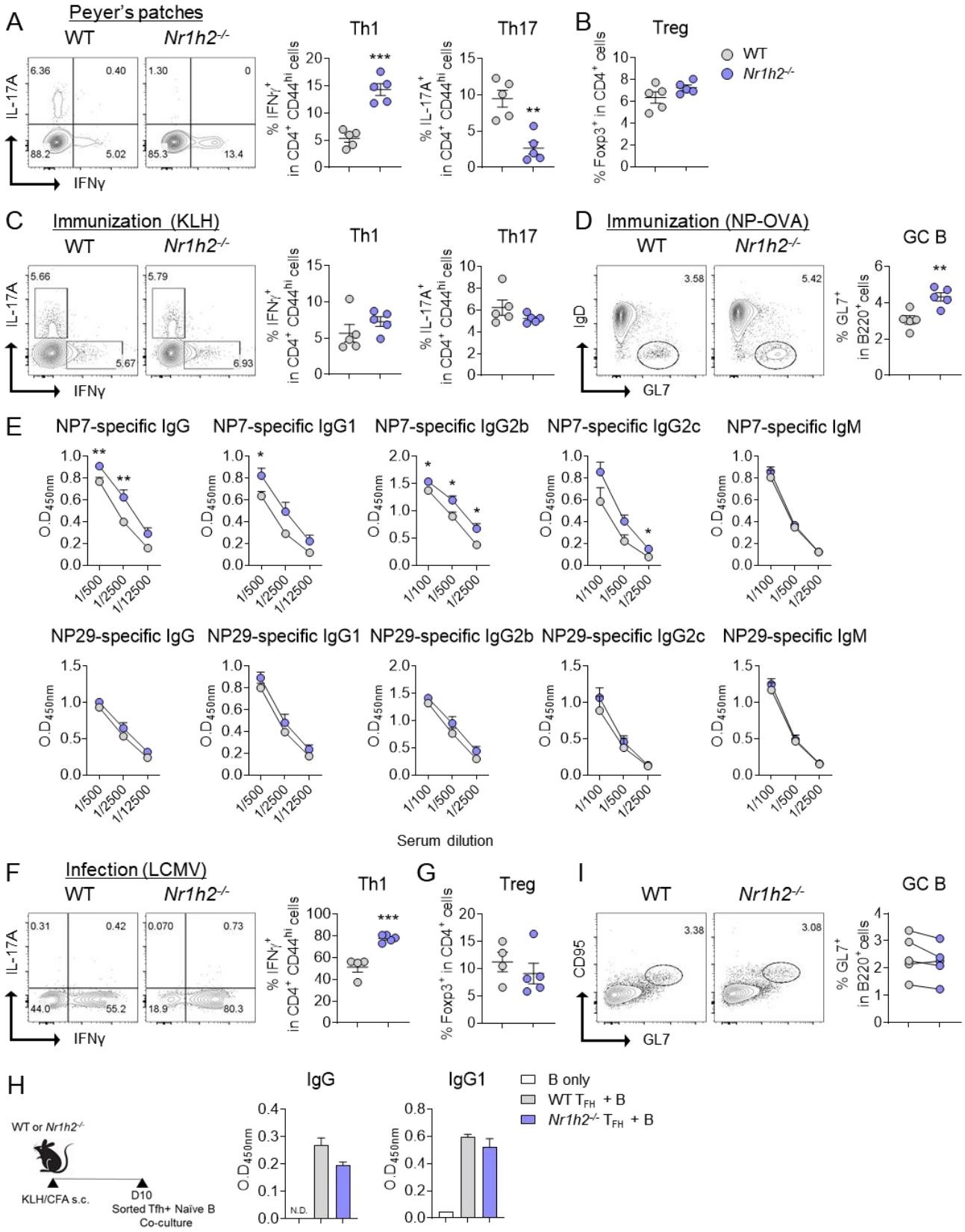
A
Peyer's patches
WT
Nr1h2-/-
IL-17A
IFNγ
6.36
0.40
88.2
5.02
1.30
0
85.3
13.4
Th1
Th17
% IFNγ+ in CD4+ CD44hi cells
% IL-17A+ in CD4+ CD44hi cells
***
**
B
Treg
% Foxp3+ in CD4+ cells
WT
Nr1h2-/-
C
Immunization (KLH)
5.66
5.67
5.79
6.93
D
Immunization (NP-OVA)
IgD
GL7
3.58
5.42
GC B
% GL7+ in B220+ cells
E
NP7-specific IgG
NP7-specific IgG1
NP7-specific IgG2b
NP7-specific IgG2c
NP7-specific IgM
NP29-specific IgG
NP29-specific IgG1
NP29-specific IgG2b
NP29-specific IgG2c
NP29-specific IgM
O.D450nm
Serum dilution
F
Infection (LCMV)
0.31
0.42
44.0
55.2
0.070
0.73
18.9
80.3
G
Treg
I
CD95
3.38
3.08
H
WT or Nr1h2-/-
KLH/CFA s.c.
D10
Sorted Tfh+ Naïve B
Co-culture
IgG
IgG1
N.D.
B only
WT TFH + B
Nr1h2-/- TFH + B

Figure S4. Helper T cell subset responses in *Nr1h2*$^{-/-}$ mice in vivo.
(A-B) Analysis of Peyer's patch at steady state (n=5). (A) Representative FACS plots and frequencies of IFNγ and IL-17A-expressing cells among CD4^{+}CD44^{hi} cells. (B) Frequencies of Treg cells. (C) WT and *Nr1h2*$^{-/-}$ mice were immunized with KLH in CFA and draining lymph nodes were analyzed on day 8. Representative FACS plots and frequencies of IFNγ and IL-17A-expressing cells among CD4^{+}CD44^{hi} cells (n=5). (D-E) WT and *Nr1h2*$^{-/-}$ mice were immunized with NP-OVA in CFA. The sera and the draining LNs were analyzed on day 8 (n=5). (D) Representative FACS plots and frequencies of GL7-expressing cells among B220^{+} cells. (E) Levels of NP_7- or NP_{29}-specific IgG, IgG1, IgG2b, IgG2c, and IgM in the serum. (F-G) WT and *Nr1h2*$^{-/-}$ mice were infected with 2×10^5 pfu of LCMV Armstrong, and spleens were analyzed on day 8 (n=4~5). (F) Representative FACS plots and frequency of IFNγ-expressing cells among CD4^{+}CD44^{hi} cells. (G) Frequencies of Treg cells. (H) BM chimeric mice were generated and immunized with KLH in CFA as in Figure 2A. Representative FACS plots and frequencies of GL7-expressing cells among B220^{+} cells in the draining LNs (n=5). (I) FACS-sorted Tfh cells and naïve B cells were co-cultured with anti-CD3 and anti-IgM for 7 days prior to Ig ELISA analysis of the culture supernatant (n=3~5). Data are representative of three independent experiments. Quantification plots show the mean ± SEM; *$p < 0.05$, **$p < 0.01$, and ***$p < 0.001$.

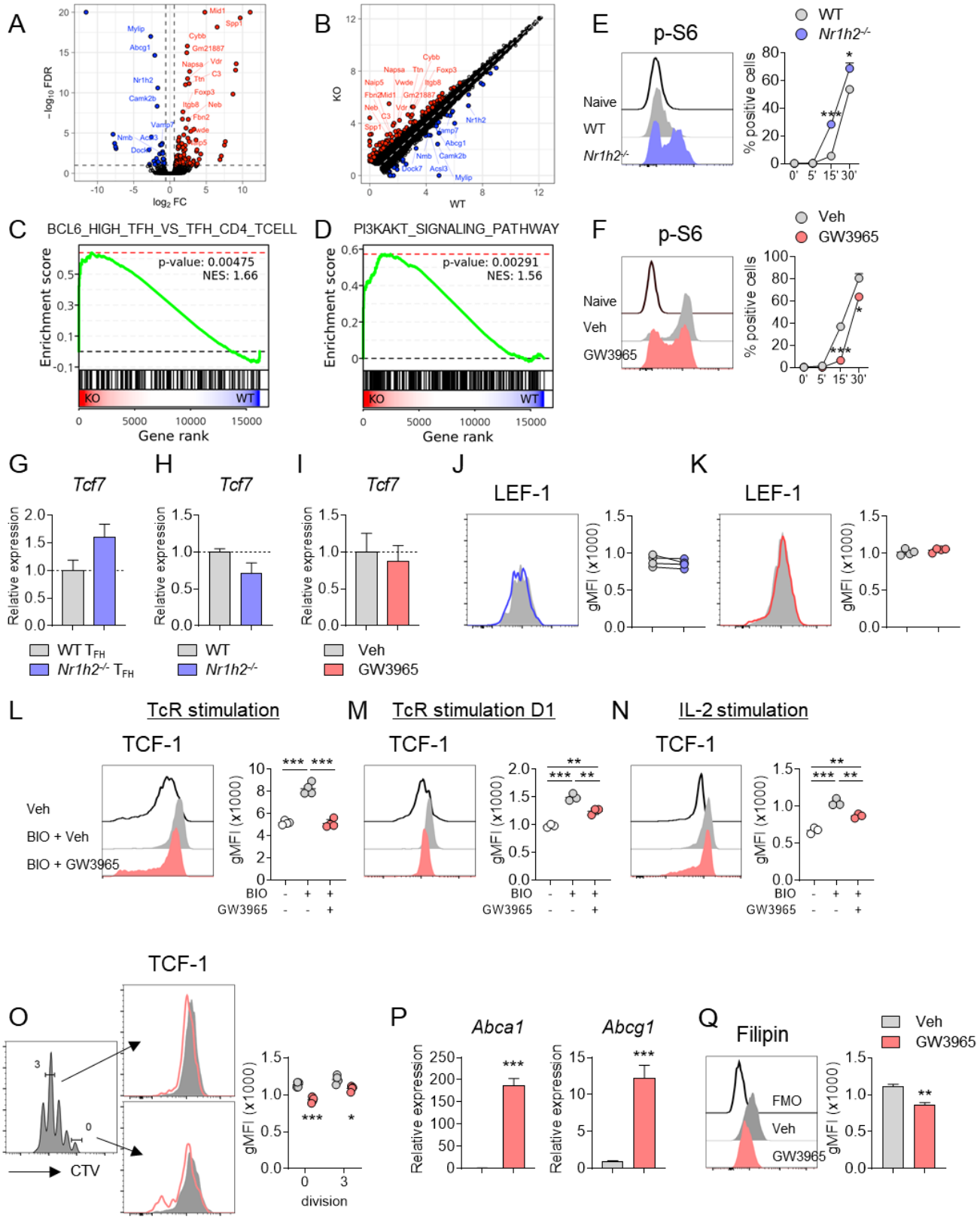
A
B
C
BCL6_HIGH_TFH_VS_TFH_CD4_TCELL
p-value: 0.00475
NES: 1.66
Enrichment score
Gene rank
KO
WT
D
PI3KAKT_SIGNALING_PATHWAY
p-value: 0.00291
NES: 1.56
E
p-S6
Naive
WT
Nr1h2-/-
% positive cells
F
Veh
GW3965
G
Tcf7
Relative expression
WT TFH
Nr1h2-/- TFH
H
I
J
LEF-1
gMFI (x1000)
K
L
TcR stimulation
TCF-1
Veh
BIO + Veh
BIO + GW3965
BIO
M
TcR stimulation D1
N
IL-2 stimulation
O
CTV
division
P
Abca1
Abcg1
Q
Filipin
FMO

Figure S5. Regulation of gene expression in Tfh cells and GSK3β-mediate TCF-1 expression in CD4$^+$ T cells by LXR.

(A-D) Tfh cells from the spleens of LCMV Armstrong-infected mice were subjected to bulk RNA-seq. (A) Volcano plot. (B) Scatter plot. (C) Geneset enrichment analysis (GSEA) of gene set, BCL6_HIGH_TFH_VS_TFH_CD4_TCELL. (D) PI3KAKT_SIGNALING_PATHWAY. (E-F) WT or *Nr1h2*$^{-/-}$ naïve CD4$^+$ T cells were stimulated with anti-CD3 and anti-CD28 in the presence of vehicle or GW3965. Representative histograms of p-S6 expressions, and frequencies of p-S6$^+$ cells (n=3). (G) Tfh cells from WT and *Nr1h2*$^{-/-}$ mice were flow-sorted and the relative expression of *Tcf7* was analyzed by qRT-PCR (n=4). (H-I) WT or *Nr1h2*$^{-/-}$ naïve CD4$^+$ T cells were stimulated with anti-CD3 and anti-CD28 in the presence of vehicle or GW3965 and analyzed for the expression of *Tcf7* (n=3). (J-K) WT or *Nr1h2*$^{-/-}$ naïve CD4$^+$ T cells were stimulated with anti-CD3 and anti-CD28 in the presence of vehicle or GW3965 and analyzed for the expression of LEF-1 (n=4). (L) Naïve CD4$^+$ T cells were stimulated with anti-CD3, anti-CD28, and BIO in the presence of vehicle or GW3965, and gMFIs of TCF-1 were examined (n=4). (M) Naïve CD4$^+$ T cells were stimulated with anti-CD3 and anti-CD28, and BIO or GW3965 were added on day 1. gMFIs of TCF-1 were examined (n=3). (N) Naïve CD4$^+$ T cells were stimulated with IL-2 and BIO in the presence of vehicle or GW3965 and gMFIs of TCF-1 were examined (n=3). (O) CTV-labeled murine naïve CD4$^+$ T cells were stimulated with anti-CD3 and anti-CD28 for 72 hours in the presence of vehicle or GW3965 before analyzing the level of TCF-1 in the cells with a similar degree of division (n=4). (P-Q) Naïve CD4$^+$ T cells were stimulated with anti-CD3 and anti-CD28 in the presence of vehicle or GW3965 (n=4). (P) Expression of *Abca1*, and *Abcg1*. (Q) Intensity of Filipin staining. Data are representative of at least two independent experiments. Quantification plots show the mean ± SEM; *$p < 0.05$, **$p < 0.01$, and ***$p < 0.001$.

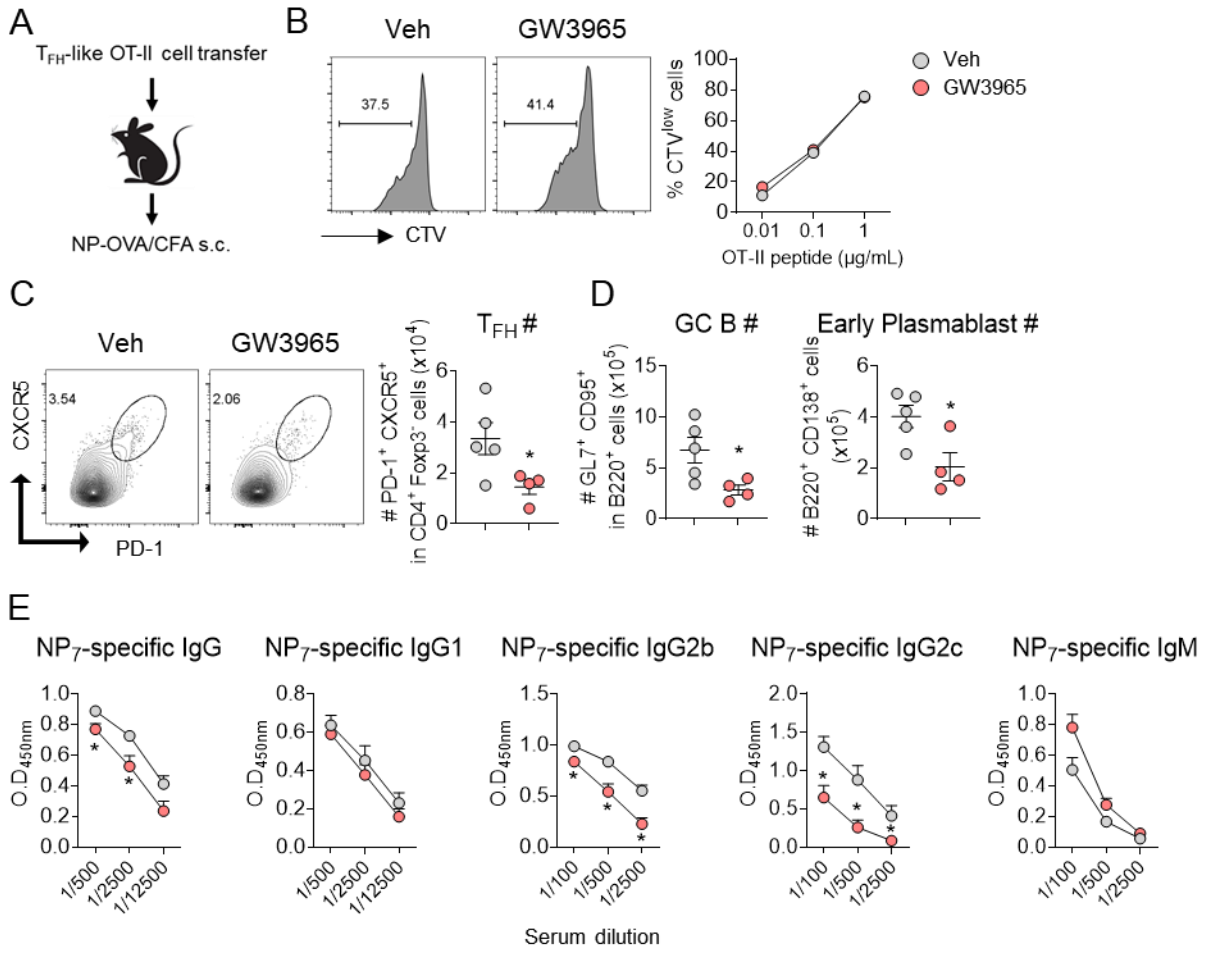

Figure S6. GW3965-treated Tfh-like cells trigger impaired germinal center reactions.
(A) Schematic representation of the Tfh-like cell adoptive co-transfer experiments (n=4~5). (B) CTV-labeled Tfh-like cells were cultured with the indicated doses of $Ova_{323-339}$ in the presence of T-cell depleted splenocytes for three days. Representative histograms of CTV expression, and frequencies of CTV^{low} cells (n=3). (C) Representative FACS plots and absolute cell numbers of Tfh cells. (D) Absolute cell numbers of germinal center B cells, and early plasmablasts. (E) Levels of NP_7-specific IgG, IgG1, IgG2b, IgG2c, and IgM in the serum. Data are representative of at least two independent experiments. Quantification plots show the mean ± SEM; *$p < 0.05$, **$p < 0.01$, and ***$p < 0.001$.

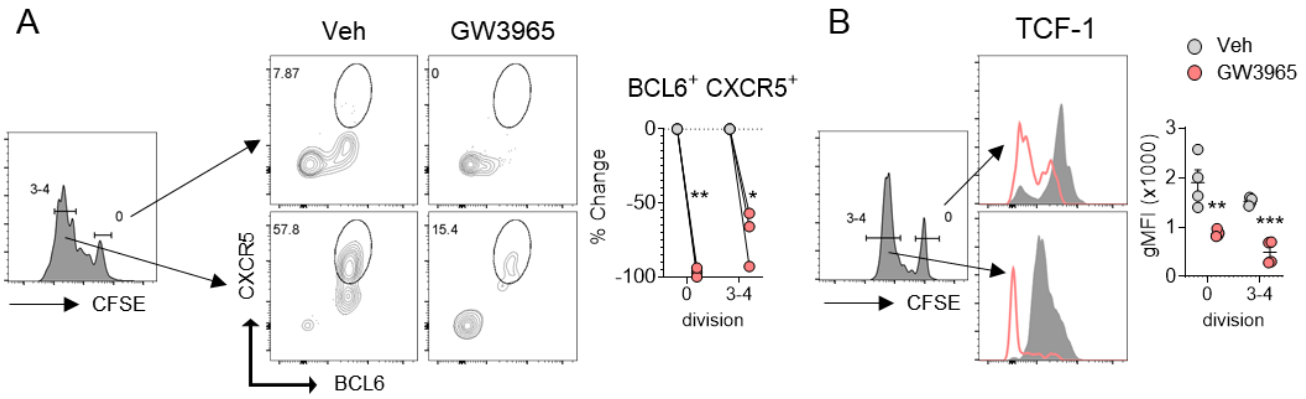

Figure S7. LXR inhibits TCF-1 expression and Tfh cell differentiation in human CD4$^+$ T cells regardless of the degree of division.

(A-B) Flow-sorted human naive CD4$^+$ T cells were CFSE-labeled and cultured under Tfh-skewing conditions in the presence of vehicle or GW3965. (A) Percentage changes in BCL6$^+$CXCR5$^+$ cells in the cells with similar degree of division as indicated (n=3). Each symbol represents an individual donor. (B) Levels of TCF-1 in the human CD4$^+$ T cells with a similar degree of division (n=4). Data are representative of three independent experiments. Quantification plots show the mean ± SEM; *p < 0.05, and ***p < 0.001.

SI REFERENCES

1. Y. U. Kim, H. Lim, H. E. Jung, R. A. Wetsel, Y. Chung, Regulation of Autoimmune Germinal Center Reactions in Lupus-Prone BXD2 Mice by Follicular Helper T Cells. *PLOS ONE* **10**, e0120294 (2015).